10700–10712 *Nucleic Acids Research, 2015, Vol. 43, No. 22* *Published online 3 September 2015*
doi: 10.1093/nar/gkv869

Directional transition from initiation to elongation in bacterial translation

Akanksha Goyal, Riccardo Belardinelli, Cristina Maracci, Pohl Milón and Marina V. Rodnina*

Department of Physical Biochemistry, Max Planck Institute for Biophysical Chemistry, 37077 Göttingen, Germany

Received July 10, 2015; Revised August 14, 2015; Accepted August 18, 2015

ABSTRACT

The transition of the 30S initiation complex (IC) to the translating 70S ribosome after 50S subunit joining provides an important checkpoint for mRNA selection during translation in bacteria. Here, we study the timing and control of reactions that occur during 70S IC formation by rapid kinetic techniques, using a toolbox of fluorescence-labeled translation components. We present a kinetic model based on global fitting of time courses obtained with eight different reporters at increasing concentrations of 50S subunits. IF1 and IF3 together affect the kinetics of subunit joining, but do not alter the elemental rates of subsequent steps of 70S IC maturation. After 50S subunit joining, IF2-dependent reactions take place independent of the presence of IF1 or IF3. GTP hydrolysis triggers the efficient dissociation of fMet-tRNA^{fMet} from IF2 and promotes the dissociation of IF2 and IF1 from the 70S IC, but does not affect IF3. The presence of non-hydrolyzable GTP analogs shifts the equilibrium towards a stable 70S–mRNA–IF1–IF2–fMet-tRNA^{fMet} complex. Our kinetic analysis reveals the molecular choreography of the late stages in translation initiation.

INTRODUCTION

Initiation of protein synthesis establishes the reading frame of the mRNA by positioning the initiator tRNA (fMet-tRNA^{fMet}) on the start codon in the P site of the ribosome. In bacteria, initiation is promoted by three initiation factors (IF1, IF2 and IF3) and entails three main phases (1–7). First, the initiation factors, fMet-tRNA^{fMet} and the mRNA are recruited to the small ribosomal subunit (30S) to form a 30S pre-initiation complex (30S PIC). In the next phase, the anticodon of fMet-tRNA^{fMet} recognizes the mRNA start codon in the P site of the 30S subunit, resulting in the formation of the 30S initiation complex (30S IC). Finally, the large ribosomal subunit (50S) associates with the 30S IC, IF2 hydrolyzes GTP to GDP and inorganic phosphate (Pi), the initiation factors are released and fMet-tRNA^{fMet} accommodates in the P site of the peptidyl transferase center ready to participate in the first peptide bond formation. The formation of the 30S IC and its maturation to the 70S elongation complex (70S EC) provide a number of kinetic checkpoints for mRNA and tRNA selection, which determine the frequency of mRNA translation in the cell (6).

The factors bind to the 30S subunit in a cooperative way, in the sense that they affect the affinity of each other's binding in the complex. IF1 increases the affinity of IF2 and IF3 towards the 30S subunit, and, in turn, IF1 is stabilized on the 30S by their presence (8–13). IF3 allosterically controls the interaction of IF2 with the 30S IC (14,15) and, together with IF1, stabilizes IF2 on the complex. *Vice versa*, the binding of IF3 to the 30S subunit is also stabilized by the presence of IF2 (13). Docking of fMet-tRNA^{fMet} to the 30S subunit occurs via specific interactions with the C2-domain of IF2 (16–18) and is followed by start codon recognition. This results in the formation of the 30S IC in which the binding of mRNA, fMet-tRNA^{fMet}, IF1 and IF2 to the 30S subunit is further strengthened, while the binding of IF3 is destabilized (13).

The conversion of the 30S IC into the 70S IC is a multistep process (Figure 1) (19–23). Synergistic positioning effect of IF2 and fMet-tRNA^{fMet} on the 30S IC drives rapid subunit association (14,24–26). One of the ways in which IF1 and IF3 influence the kinetics of 50S docking is by modulating the orientation and dynamics of IF2–GTP–fMet-tRNA^{fMet} complex on the 30S IC (15,26,27). In addition, IF3 sterically hinders the formation of intersubunit bridges (27,28), thereby slowing down 50S subunit docking. Together, IF1 and IF3 help to discriminate against incorrectly formed 30S ICs, such as those programmed with an mRNA containing a non-optimal translation initiation region (TIR) or lacking IF2 or fMet-tRNA^{fMet}, by inducing a conformation of the 30S IC which impedes 50S subunit joining (21,24,29–31).

The current model for 70S IC formation – based on biochemical, rapid kinetic, and single-molecule FRET studies – suggests that 50S subunit joining triggers rapid GTP hydrolysis by IF2, leading to a series of ribosome and IF2 conformational changes and fMet-tRNA^{fMet} move-

*To whom correspondence should be addressed. Tel: +49 551 201 2900; Fax: +49 551 2905; Email: rodnina@mpibpc.mpg.de
Present address: Pohl Milón, School of Medicine, Faculty of Health Sciences, Universidad Peruana de Ciencias Aplicadas - UPC, Lima, L-33, Perú.

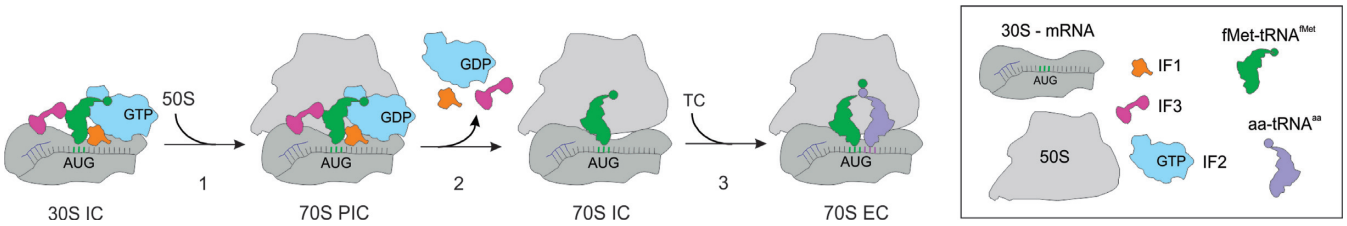

Figure 1. Schematic of late events in bacterial translation initiation. IF1, IF2–GTP, IF3, mRNA and fMet-tRNA^{fMet} bind the 30S subunit to form a 30S IC. Phase 1: Association of the 50S subunit to 30S IC triggers rapid GTP hydrolysis by IF2 and forms a 70S pre-initiation complex (70S PIC). Phase 2: Dissociation of IF1, IF2 and IF3 from the ribosome results in an elongation-ready 70S IC. Phase 3: Binding of EF-Tu–GTP–aminoacyl-tRNA (ternary complex, TC) to the 70S IC is followed by peptide bond formation, resulting in a 70S elongation complex (70S EC).

ments (19,20,23,32–34). The fMet-tRNA^{fMet} is released from the C2-domain of IF2 into the canonical P/P site (26,27,33,34), and the subunits rotate with respect to one another into the classical state, allowing the ribosome to enter an elongation-competent conformation (22). Finally, IF2 presumably dissociates from the 70S complex (33–37), allowing the aminoacyl-tRNA in the ternary complex with EF-Tu and GTP (TC) to bind to the A site and form the first peptide bond. IF3 dissociation from the ribosome also follows subunit joining, as demonstrated by rapid kinetics (21), chemical probing (38), and single-molecule FRET (15,39).

The interplay between IF1, IF2 and IF3 upon transition from the 30S IC to the 70S IC is poorly understood. Reactions such as IF1 dissociation from the 70S complex, the loss of direct interaction between fMet-tRNA^{fMet} and the C2-domain of IF2, and the dissociation of GDP from IF2, have not been monitored directly yet. Previous studies have suggested that IF1 and IF2 interact on the 30S IC (13,27,40,41) and may affect each other's release from the ribosome. The movements of fMet-tRNA^{fMet} have been studied using a fluorescence reporter at the elbow region of tRNA^{fMet}(Prf20) (20,23), but it is not certain whether the fluorescence changes of Prf20 represent the dissociation of tRNA^{fMet} from IF2, the accommodation of the 3′ CCA-end in the 50S P site, or some other rearrangement. Finally, the role of GTP hydrolysis by IF2 during initiation, as studied using different non-hydrolyzable GTP analogs, is controversial because the results of the experiments seem to depend on the analog used and the source of initiation components – *Escherichia coli* or *Geobacillus stearothermophilus* (20,23,33,34,36). Here we examine the late events of translation initiation using a homologous system of translation initiation components from *E. coli* (42) and a toolbox of novel fluorescence reporters. The results provide a comprehensive kinetic scheme for maturation of 70S PIC into an elongating 70S complex, including the timing and control of dissociation of IF1 and IF2. Our results give insights into the interplay between the initiation factors and underscore the role of IF2 and GTP hydrolysis during translation initiation.

MATERIALS AND METHODS

Preparation of components

Ribosomal subunits were prepared by zonal centrifugation from 70S ribosomes purified from *E. coli* MRE600 (42,43). 30S subunits were reactivated in buffer A (50 mM Tris–HCl [pH 7.5], 70 mM NH_4Cl, 30 mM KCl, 7 mM $MgCl_2$) with additional 14 mM $MgCl_2$ for 30 min at 37°C. EF-Tu, IF1 and IF3 were prepared as described (42,44). IF2 and truncated mutants of IF2 (ΔN (lacking residues 1–294) and ΔC2 (lacking residues 792–890)) were prepared by Ni-NTA affinity chromatography. fMet-tRNA^{fMet} was purified by HPLC (42) and was 95% aminoacylated and formylated. 022 mRNA (42) was prepared by T7 RNA polymerase transcription. GTP, GDP, GTPγS, GDPNP, mant-GTP (2′/3′-*O*-(*N*-methyl-anthraniloyl)-guanosine-5′-triphosphate, triethylammonium salt) and mant-GTPγS (2′/3′-*O*-(*N*-methyl-anthraniloyl)-guanosine-5′-(γ-thio)-triphosphate, triethylammonium salt), were purchased from Jena Biosciences; Bpy-GTP (guanosine 5′-triphosphate, BODIPY FL 2′-(or-3′)-*O*-(*N*-(2-aminoethyl)urethane), trisodium salt) and Bpy-GDP (guanosine 5′-diphosphate, BODIPY FL 2′-(or-3′)-*O*-(*N*-(2-aminoethyl)urethane), bis-(triethylammonium) salt) from Life Technologies.

Fluorescence labeling of single cysteine mutant IF1 with thiol-reactive dyes (Alexa(Alx)555 and Atto540Q maleimides) was performed according to published protocols (13,21,42). Preparation of $30S_{S13}$(Alx488) subunits by reconstitution of 30SΔS13 with fluorescence-labeled $S13_{112}$(Alx488) was carried out as described (45,46). Fluorescence labeling of *E. coli* phosphate-binding protein (PBP; (47)) and Met-tRNA^{fMet} (48,49) was carried out as described. The efficiency of labeling, assessed by SDS-PAGE and spectrophotometric analysis was >80%.

Biochemical methods

The 30S IC (0.1–0.3 μM) was formed by incubating 30S subunits with a 3-fold excess of IF2, IF3 and IF1 (or 2-fold excess of labeled IF1), and a 5-fold excess of mRNA and f[^{3}H]Met-tRNA^{fMet} (or 3-fold excess of Bpy-Met-tRNA^{fMet}) in buffer A, containing 0.25 mM GTP (or 4 μM Bpy-GTP/10 μM mant-GTP) for 30 min at 37°C. Ternary complex EF-Tu–GTP–Phe-tRNA^{Phe} was prepared by incubating EF-Tu (1.6 μM) with Phe-tRNA^{Phe} (0.8 μM) and GTP (0.25 mM), in the presence of phosphoenol pyruvate (2 mM) and pyruvate kinase (0.1 μg/μl) for 15 min at 37°C.

Purified 70S IC with Bpy-Met-tRNA^{fMet} was prepared by incubating 70S ribosomes (1 μM) in the presence of initiation factors (1.5 μM), 022 mRNA (2 μM), Bpy-[H^3]Met-tRNA^{fMet} (1.5 μM) and GTP (0.25 mM) at 37°C for 1 h. 1.4 ml of the reaction mix was layered on top of 600 μl of 1.1 M sucrose in buffer A. Complexes were centrifuged for 4 h at 55 000 rpm (rotor TLS-55 in Beckman Coulter ultra-

centrifuge). Pellets were dissolved in buffer A. The concentration of ribosomes and the efficiency of 70S IC formation was checked by measuring the absorbance at 260 nm and radioactivity of Bpy-[^{3}H]Met-tRNA^{fMet}.

Kinetic experiments

All measurements were carried out in buffer A at 20°C. Stopped-flow measurements were performed using a SX-20MV stopped-flow apparatus (Applied Photophysics, Leatherhead, UK) by rapidly mixing equal volumes (60 μl each) of 30S IC (0.05–0.15 μM final concentration) and 50S subunits added in increasing concentrations (0–2 μM). All experiments were carried out at pseudo-first order conditions, i.e. at least at a 3-fold excess of 50S subunits over 30S ICs. No significant amplitude dependence was observed upon increasing 50S concentration and thus the time courses were normalized with respect to amplitude changes to facilitate visual comparison of time courses (Figure 2). In experiments performed in the absence of IF1 and IF3, light scattering (LS) (see below) was measured at increasing 50S concentrations (0.15–0.5 μM), but all other experiments were carried out at a fixed concentration of 50S subunits (1 μM). The experiments with GTPγS were carried out at 1 μM 50S subunits.

LS and IF3 dissociation were measured as described (21). To measure LS, the excitation wavelength was set to 434 nm, and the scattered light was measured at an angle of 90° to the incident beam without a filter. Direct excitation of Alx555 was at 555 nm and the output was monitored after passing through cut-off filter KV590 (Schott). Direct excitation of Bpy and Alx488 was at 470 nm and the output was monitored after passing through a KV500 cut-off filter. Pi release was monitored using fluorescent MDCC-PBP protein (2 μM) and a Pi-MOP mixture (0.1 U/ml PNPase and 200 μM 7-methylguanosine) (47) in the presence of GTP (10 μM). Direct excitation of MDCC was at 425 nm and the output was monitored after passing through a KV450 cut-off filter. FRET between the intrinsic Trp residue of IF2 and mant-GTP was monitored by mant emission passing through a KV408 cut-off filter upon excitation at 290 nm. Dipeptide formation was measured in a quench-flow apparatus (KinTek) and the extent of f[^{3}H]Met-[^{14}C]Phe dipeptide formation was determined by HPLC and liquid scintillation counting. Binding of Bpy-GTP and Bpy-GDP to IF2 was monitored by rapidly mixing Bpy-GTP or Bpy-GDP (2 μM) with free IF2 (0.1 μM) or IF2 bound to 30S IC (0.1 μM), formed in the absence of any nucleotide, in the stopped-flow apparatus.

IF2 release from, and subsequent re-association with, 70S IC was measured by rapidly mixing 30S IC (0.05 μM) formed in the presence of Bpy-Met-tRNA^{fMet} and GTP (12.5 μM), with 50S subunits (0.25 μM), IF2 (4 μM) and GTPγS (0.25 mM). IF1 release from, and re-association with 70S IC, was measured by rapidly mixing 30S$_{S13}$(Alx488) IC (0.05 μM) formed in the absence of IF3, but in the presence of IF1$_4$(Atto540Q) and GTP (12.5 μM), with 50S subunits (0.25 μM) and GTPγS (0.25 mM).

Binding of IF2 to 70S IC was measured by rapidly mixing purified 70S IC (containing Bpy-Met-tRNA^{fMet}) (10 nM) with IF2 (4 μM) bound to different GTP analogs

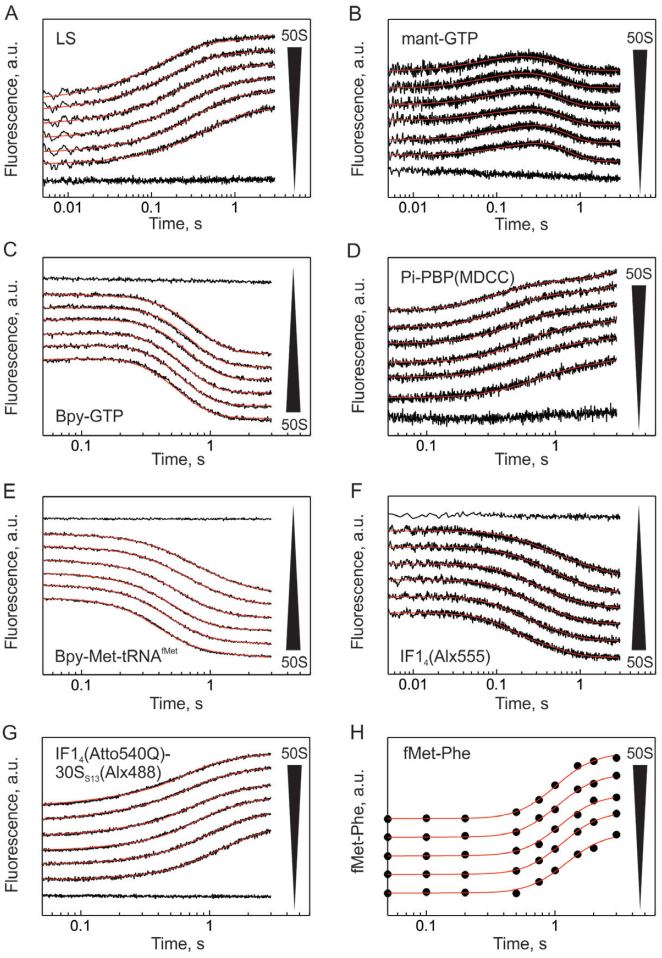

Figure 2. Time courses of reactions during 70S IC maturation. 30S IC, formed in the presence of indicated fluorescence-labeled initiation components, was rapidly mixed with increasing concentrations of 50S subunits in a stopped-flow (A–G) or a quench-flow (H) machine. (**A**) Time courses of 50S subunit joining. (**B**) Time courses of GTPase activation and IF2 release. (**C**) Time courses of GDP dissociation. (**D**) Time courses of Pi release from IF2. (**E**) Time courses of tRNA^{fMet} release from IF2 into the ribosomal P site. (**F**) Time courses of change in IF1 environment on the 70S IC. (**G**) Time courses of IF1 dissociation. (**H**) Time courses of the first fMet-Phe peptide bond formation. Type of observable and the variation in 50S subunit concentrations (0–2 μM) are indicated. The traces were normalized with respect to amplitude changes. Smooth lines show fits obtained by global evaluation of all time courses using numerical integration.

(0.25 mM). To measure the binding of IF1$_4$(Atto540Q) to 70S$_{S13}$(Alx488) IC, 70S complexes were prepared from 30S$_{S13}$(Alx488), IF2, 022 mRNA, fMet-tRNA^{fMet}, 50S subunits and GTP (12.5 μM). Unpurified 70S$_{S13}$(Alx488) ICs were rapidly mixed with IF1$_4$(Atto540Q) and GTP/GTPγS (0.25 mM) in the stopped-flow apparatus.

Kinetic modeling

Time courses of Bpy-GTP and Bpy-GDP binding to IF2, Bpy-Met-tRNA^{fMet} binding to 30S PIC, IF2 binding to 70S IC containing Bpy-Met-tRNA^{fMet}, IF1$_4$(Atto540Q) binding to 70S$_{S13}$(Alx488), IF1 chase from the 30S IC and IF3 dissociation from the 70S IC were evaluated using exponential fitting. Time courses of reactions on the 70S IC were

collectively evaluated by numerical integration using a 9-step model (see Results). For Pi release and FRET between mant-GTP and IF2, the fit of the buffer control trace (obtained in the absence of 50S subunits) was subtracted from the respective time courses obtained in the presence of 50S subunits. Time courses for the observables which displayed a signal change in the presence of GTPγS were fitted with a 4-step model (A→B (LS); B→C (mant-GTPγS); C→D ($IF1_4$(Alx555)) and D→E (slow subunit joining)). All calculations were performed using Prism (Graphpad Software) and KinTek Explorer (KinTek corporation, USA). Standard errors were calculated from fitting of the average time course derived from 7–10 technical replicates of each reaction. Statistics of the global fits are presented in Supplementary Materials.

RESULTS

Observables and step assignment

30S ICs were prepared using purified initiation components from *E. coli*. As a model mRNA, we chose m022, because the 30S IC formed with this mRNA allows rapid subunit joining (20,21), which is essential to resolve the individual rates of the subsequent reactions. To monitor the transition from 30S IC to 70S IC, we started the reaction by rapidly mixing pre-formed 30S IC with 50S subunits. The timing of several processes which occur after 50S subunit joining was determined using fluorescence-labeled components, following fluorescence intensity or Förster resonance energy transfer (FRET) changes with time (Figure 2). We utilized novel observables to follow the kinetics of IF1 dissociation from the 70S complex, as well as IF2-dependent reactions such as the dissociation of the fMet-$tRNA^{fMet}$ CCA-end and GDP release from IF2. We also monitored previously reported reactions such as subunit joining, Pi release from IF2, and peptide bond formation (19–21,50) to formulate a comprehensive kinetic model that included all reactions.

The activity of each fluorescent component in promoting IC formation was assessed by measuring subunit joining, monitoring light scattering (LS). The kinetics of subunit association remained unaffected in each case (Supplementary Figure S1A), indicating that the labeling did not appreciably alter the functional characteristics of the 30S IC. To assign the order and timing of the respective steps, the time courses were initially evaluated by exponential fitting. Where possible, the sequence of events was assigned based on apparent rate constants (Table 1). As a second criterion, the sequence was assessed based on the length of the delay phase preceding the respective reaction (Supplementary Figure S2). Subsequently, the rate constants of the elemental reactions were obtained by numerical integration using the combined datasets for all reporters (Table 2).

Association of the 50S subunit with the 30S IC (Figure 2A) (21) resulted in a biphasic change of LS, with the predominant (>65% of the total amplitude change) rapid phase indicative of 50S joining to the majority of 30S ICs which were present in a 'productive' conformation, and a minor phase which probably represents a small portion of less active (51) or compositionally heterogeneous complexes. The initial evaluation of the LS kinetics was performed by exponential fitting, which showed that the apparent rate constant (k_{app}) of the predominant step increased linearly with the 50S subunit concentration (15 $\mu M^{-1}s^{-1}$; Table 1) (Supplementary Figure S1B), indicative of a bimolecular association step, in agreement with previous reports (20,21).

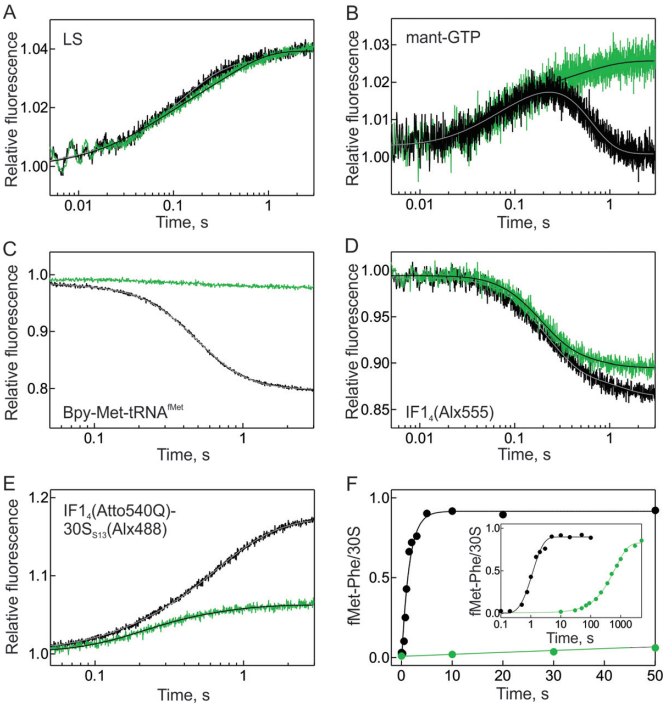

Figure 3. Effect of GTP hydrolysis on the kinetics of 70S IC maturation. 30S IC was rapidly mixed with 50S subunits (1 μM) in a stopped-flow (**A**–**E**) or a quench-flow (**F**) machine and the time courses of indicated reactions were monitored in the presence of GTP (black) or GTPγS (green). An inset in (**F**) shows the extended time window for peptide bond formation. Smooth lines (A–E) show fits obtained by global evaluation of all time courses using numerical integration.

Next, we sought to study the reactions linked to IF2. The interaction of GTP with the G-domain of IF2 was monitored using the fluorescent GTP analogs mant-GTP and Bodipy (Bpy)-GTP. We followed FRET between mant-GTP and the intrinsic Trp residue of the factor (52,53). The kinetics of mant-GTP binding to and dissociation from IF2, reported previously, indicated that the affinity of IF2 for mant-GTP is in the same range as that for non-fluorescent GTP (52,54). Upon 50S joining to 30S ICs formed with mant-GTP, a biphasic FRET change was observed (Figure 2B). The apparent rate constants of both phases displayed a hyperbolic dependence on increasing 50S concentration (Supplementary Figure S1C) and saturated at 9 s^{-1} and 2.5 s^{-1} (Table 1), indicating that the two reactions represent rearrangements of IF2 which follow the bimolecular subunit joining step. When mant-GTP was replaced with a non-hydrolyzable analog, mant-GTPγS, the first step was not affected (Figure 3B), suggesting that the respective rearrangement of the IF2 G-domain occurs in the pre-hydrolysis state of the factor. The second step, however, displayed a strong dependency on GTP hydrolysis and was abolished in the presence of GTPγS. In accordance with similar results obtained with EF-Tu (55–57), we assigned the first,

Table 1. Summary of the apparent rate constants of reactions during 70S IC maturation

Kinetic step	Observable	All IFs GTP[a]	–IF1 GTP[b]	–IF3 GTP[b]	All IFs GTPγS[c]
Subunit joining, $k_{app\ on}$ ($\mu M^{-1}\ s^{-1}$)	LS (>65%)	14 ± 1	38 ± 4	37 ± 4	n.d.
GTPase activation (s^{-1})	Mant-GTP	9.1 ± 0.5	14 ± 1	27 ± 1	7.4 ± 0.5
Change of IF1 environment (s^{-1})	$IF1_4$(Alx555) (>80%)	4.7 ± 0.5	n.o.	9.7 ± 0.5	3.7 ± 0.5
IF1 dissociation (s^{-1})	$IF1_4$(Atto540Q) – $30S_{S13}$(Alx488) (>60%)	1.9 ± 0.1	n.o.	2.1 ± 0.1	n.o.
IF2 dissociation (s^{-1})	Mant-GTP	2.5 ± 0.1	2.8 ± 0.1	2.3 ± 0.1	n.o.
IF3 dissociation (s^{-1})	$IF3_{166}$(Alx555) – $fMet\text{-}tRNA^{fMet}$ (Flu)[d]	3.2 ± 0.1	9.6 ± 0.3	n.o.	2.9 ± 0.1

All rates are derived from exponential fitting of time courses. In case of double-exponential fitting, the amplitude contribution of the relevant phase is presented in brackets as % of the total amplitude change. For mant-GTP, the fluorescence change has an upward (GTPase activation) and downward (IF2 dissociation) phase and therefore the amplitude contributions are not indicated. Values are represented as mean ± SEM; n.d. – not determined; n.o. – not observed. See also Supplementary Figure S1.
[a]For 30S ICs formed with all IFs and GTP, time courses were measured at five to six different 50S subunit concentrations for each observable.
[b]For –IF1 and –IF3, LS was monitored at varying 50S concentrations. For each of the remaining observables, single time courses were obtained at 1 μM 50S subunit concentration.
[c]For GTPγS, a single time course for each of observable was obtained at 1 μM 50S subunit concentration.
[d]Single-exponential fitting.

Table 2. Summary of the elemental rate constants of reactions during 70S IC maturation

Kinetic step	Observable	All IFs GTP[a]	–IF1 GTP[b]	–IF3 GTP[b]	All IFs GTPγS[c]
50S association, k_1 ($\mu M^{-1}s^{-1}$)	LS	29 ± 6	43 ± 5	51 ± 5	23 ± 6
50S dissociation, k_{-1} (s^{-1})	LS	29 ± 15	~0	5 ± 3	13 ± 10
GTPase activation, k_2 (s^{-1})	Mant-GTP	36 ± 6	23 ± 5	$>k_1$[d]	37 ± 10
Change of IF1 environment, k_3 (s^{-1})	$IF1_4$(Alx555)	21 ± 5	n.o.	13 ± 1	11 ± 3
Pi release, k_4 (s^{-1})	Pi-PBP(MDCC)	3.7 ± 0.5	4.1 ± 0.5	4.0 ± 0.5	n.o.
$fMet\text{-}tRNA^{fMet}$ release from IF2, k_5 (s^{-1})	$Bpy\text{-}Met\text{-}tRNA^{fMet}$	18 ± 5	13 ± 3	13 ± 3	n.o.
IF2 and GDP release, k_6 (s^{-1})	Mant-GTP and Bpy-GTP	6.0 ± 0.5	as k_5 and 7.4 ± 0.6	as k_5 and 7 ± 1	n.o.
IF1 dissociation, k_6 (s^{-1})	$IF1_4$(Atto540Q)-$30S_{S13}$(Alx488)	6.0 ± 0.5	n.o.	7 ± 1	n.o.
Peptide bond formation, k_7 (s^{-1})	fMet-Phe	2.3 ± 0.8	3 ± 1	4 ± 2	n.o.

All rates are derived from global fitting of collective time courses using numerical integration. Values derived from global fitting are represented as mean ± SEM; n.o., not observed.
[a]For 30S ICs formed with all IFs and GTP, time courses were measured at five to six different 50S subunit concentrations for each observable.
[b]For –IF1 and –IF3, the concentration dependence for LS was combined with a single time course (obtained at 1 μM 50S subunit concentration) for each of the remaining observables.
[c]Because there was no difference between the rates of LS obtained with GTP or GTPγS (Figure 3A), the concentration dependence for the LS (GTP), was combined with single time courses (obtained at 1 μM 50S subunit concentration) for mant-GTPγS and $IF1_4$(Alx555)(GTPγS).
[d]The kinetics of GTPase activation are indistinguishable from 50S subunit joining.

upward phase to GTPase activation and the second, downward phase to IF2 dissociation from the 70S complex, although we cannot exclude that the second phase may represent the release of the nucleotide from IF2 or a conformational rearrangement of the factor upon dissociation from the ribosome.

When Bpy-GTP was used to form the 30S IC, the Bpy fluorescence decreased after a lag phase of ~200 ms following the 50S subunit joining (Figure 2C). To identify the cause of the fluorescence change, we monitored the interaction of Bpy-GTP and Bpy-GDP with free or 30S-bound IF2 (Supplementary Figure S3). The fluorescence increase upon Bpy-GTP or Bpy-GDP binding to IF2 (Supplementary Figure S3A–C), and the fluorescence decrease upon chase with non-fluorescent GTP (Supplementary Figure S3D) was equivalent in amplitude to the fluorescence change observed during 70S IC formation. On the basis of these results we concluded that the decrease in fluorescence of Bpy-nucleotide observed upon 70S IC formation reports on the release of Bpy-GDP from IF2 after hydrolysis of Bpy-GTP. Because the final concentration of Bpy-GDP in the reaction, after hydrolysis of Bpy-GTP, is determined by the concentration of the 30S IC (0.1 μM), which is at least 10-fold lower than the K_d of GDP binding to free-IF2 (~1–2 μM (58)), the dissociation of Bpy-GDP from IF2 is expected to be spontaneous.

To monitor Pi release from IF2 after GTP hydrolysis, we used an indicator reaction where the fluorescent derivative of phosphate-binding protein, MDCC-PBP, rapidly binds Pi released from IF2. We observed a biphasic increase of fluorescence following a ~75 ms delay (Figure 2D) (19,47). Single turnover Pi release, which resulted in the major fluorescence change, was followed by a slow step representing subsequent multiple turnover events of GTP hydrolysis. In the absence of 50S subunits, no change in fluorescence was observed due to the low levels of intrinsic GTPase activity of IF2 (32,59).

The dynamics of the 3′ end of $tRNA^{fMet}$ were monitored using a Bodipy-FL label attached to the amino group of Met ($Bpy\text{-}Met\text{-}tRNA^{fMet}$) (48). The position of the fluorophore allowed us to monitor the interaction of the 3′ CCA-end of $Bpy\text{-}Met\text{-}tRNA^{fMet}$ with the C2-domain of

IF2. Bpy-Met-tRNA^{fMet} fluorescence increased upon its recruitment to the 30S PIC by IF2 (Supplementary Figure S4). No fluorescence change was observed in the absence of IF2, 30S or when a truncated mutant of IF2 lacking the C2-domain (IF2ΔC2) was used instead. Upon 50S docking to the 30S IC, a ∼100 ms lag phase was followed by a decrease in fluorescence, which we attribute to the release of tRNA^{fMet} from IF2 during 70S IC formation (Figure 2E) (33,34).

The timing of IF1-dependent rearrangements is not known. To monitor the dynamics of IF1 after 50S subunit joining, we used an IF1 variant containing a cysteine residue engineered at position 4 and labeled with either the fluorescent dye Alexa555 (IF1$_4$(Alx555)) (13,42) or the quencher Atto540Q (IF1$_4$(Atto540Q)). The interaction of IF1 with the ribosome was studied with the help of two reporters, monitoring (i) the fluorescence change of IF1$_4$(Alx555) and (ii) the FRET change between Alx488 attached at residue 112 of ribosomal protein S13 on the 30S subunit (30S$_{S13}$(Alx488)) and IF1$_4$(Atto540Q) (45,46). When IF1$_4$(Alx555) bound to the 30S IC was chased by an excess of the non-fluorescent factor, a ∼15% decrease in fluorescence occurred with a rate of ∼0.03 s^{-1} (Supplementary Figure S5A). The chase of IF1$_4$(Atto540Q) from 30S$_{S13}$(Alx488) led to a ∼20% increase in fluorescence due to the spatial separation of the two dyes upon IF1 dissociation and proceeded in two steps — one step with a small FRET change (∼20% of the total amplitude change) which took place with a rate of ∼0.025 s^{-1} (similar to the rate of fluorescence change by IF1$_4$(Alx555)), and a slower step (0.01 s^{-1}) that accounted for most of the FRET signal change (Supplementary Figure S5B). When 50S subunits were mixed with 30S IC formed with IF1$_4$(Alx555) (Figure 2F) or with the FRET pair IF1$_4$(Atto540Q) and 30S$_{S13}$(Alx488) (Figure 2G), the amplitude change in each case was similar to the respective amplitude observed during the chase of the factor from the 30S complex (Supplementary Figure S5A-B), indicating that 50S joining promotes complete dissociation of the factor from the 70S complex. The k_{app} obtained by exponential fitting of time courses of the two reactions showed a hyperbolic dependence on 50S subunit concentration (Supplementary Figure S1D), saturating at 4.7 and 1.9 s^{-1}, respectively (Table 1). These results suggested that IF1 dissociation from the 30S complex and 70S complex may proceed via a two-step mechanism, with the first step reported by the fluorescence changes of IF1$_4$(Alx555) and the second step reported by the change of FRET between 30S$_{S13}$(Alx488) and IF1$_4$(Atto540Q).

The distinction between the two observables was further supported by experiments monitoring 70S IC formation in the presence of GTPγS (Figure 3D-E): the fluorescence change of IF1$_4$(Alx555) was not affected, whereas the FRET between 30S$_{S13}$(Alx488) and IF1$_4$(Atto540Q) was largely inhibited (see below), indicating that the two observables reported on two different reactions. Because IF1 is a relatively small, tightly folded protein, it is unlikely that the fluorescence intensity change of IF1$_4$(Alx555) reflects a structural rearrangement of the factor itself. Rather, the fluorescence change may reflect an alteration in the environment of the reporter owing to a conformational rearrangement of the complex or establishment of alternative IF1 contacts (30) (in the following text, we refer to this step as 'change of IF1 environment'). On the other hand, the loss of FRET between IF1$_4$(Atto540Q) and 30S$_{S13}$(Alx488), which leads to an increase of donor fluorescence, can be attributed to the subsequent dissociation of IF1 from the 70S complex.

Finally, to monitor the transition of the 30S IC into the elongation-competent 70S IC, dipeptide formation was measured by quench-flow. 30S ICs were rapidly mixed with 50S subunits and EF-Tu–GTP–Phe-tRNA^{Phe}, and fMet-Phe formation was followed over time (Figure 2H).

Replacement of GTP with GTPγS

The requirement for GTP hydrolysis by IF2 in promoting different reactions was examined by substituting GTP with a non-hydrolyzable GTP analog, GTPγS. Recent studies on eIF5B, the eukaryotic homolog of IF2, have deemed GTPγS as a suitable GTP analog due to its ability to correctly coordinate a monovalent cation in the active site (60). Similar conclusions were reached for SelB (61) where GTPγS was shown to be an authentic GTP analog. In agreement with previous reports, the replacement of GTP with GTPγS on the 30S complex did not affect subunit joining (Figure 3A and Table 1) (23,36,62,63). When mant-GTP was replaced by mant-GTPγS, only the first phase of fluorescence increase, reporting GTPase activation, was observed (Figure 3B and Table 1). The second phase, indicative of IF2 dissociation, was blocked, in agreement with previous reports suggesting that GTP hydrolysis is required for IF2 release from the 70S IC (20,33–36). GTP hydrolysis was also essential for tRNA^{fMet} release from the C2-domain of IF2, as the replacement of GTP with GTPγS completely abolished that reaction (Figure 3C).

As mentioned above, the two observables used to monitor IF1 dynamics on the 70S IC responded differently to the lack of GTP hydrolysis, suggesting that the reporters account for two separate rearrangements. The absence of GTP hydrolysis did not significantly affect the change in IF1 environment, as reported by IF1$_4$(Alx555) (Figure 3D and Table 1), but IF1 dissociation from the 70S complex – as monitored by IF1–30S FRET – was largely prevented (Figure 3E). We checked whether a similar effect was seen for IF3 dissociation by monitoring FRET between IF3$_{166}$(Alx555) and fluorescein-labeled fMet-tRNA^{fMet} (21), and found the dissociation of IF3 to be entirely independent of GTP hydrolysis (Supplementary Figure S6).

Peptide bond formation was inhibited when GTP hydrolysis was prevented (Figure 3F), indicating that GTP hydrolysis by IF2 is required for the productive transition of the 70S IC into an elongation-competent state. Assuming that 70S maturation into an elongation-ready state is limited by GTPγS hydrolysis and subsequent IF2 dissociation, dipeptide formation can be used as an indicator to provide an estimate for the rate of hydrolysis of GTPγS by IF2 (0.0015 s^{-1}) (Figure 3F (inset)).

Timing of late initiation events

To solve the kinetic mechanism, each reaction was monitored at increasing concentrations of 50S subunits (Figure 2). We determined the rate constants of elemental reactions from the global fitting of time courses for all observables to provide a comprehensive solution for processes involved in 70S IC formation. By comparing apparent rate constants (Table 1), the delay phase of time courses (Supplementary Figure S2A), and the dependence of different reactions on GTP hydrolysis (Figure 3), we formulated the following 9-step model to evaluate the time courses of reactions:

$$A + R \underset{k_{-1}}{\overset{k_1}{\leftrightarrow}} B \xrightarrow{k_2} C \xrightarrow{k_3} D \xrightarrow{k_4} E \xrightarrow{k_5} F \xrightarrow{k_6} G \xrightarrow{k_7} H \xrightarrow{k_8} I \xrightarrow{k_9} J$$

where A and R refer to the 30S IC and 50S subunit, respectively, and B to J are intermediates on the pathway from the 30S IC to 70S EC formation. The kinetics of subunit joining are described by k_1 and k_{-1}. The first phase of FRET change between mant-GTP and a Trp residue in IF2 (GTPase activation) corresponds to the B→C transition (rate constant k_2) because – based on the exponential fitting – it is the fastest rearrangement step which is independent of GTP hydrolysis. The transition C→D (k_3) is assigned to the change of IF1 environment which is independent of GTP hydrolysis and is predominantly shown by the fluorescence changes of $IF1_4$(Alx555) (major part of the reaction amplitude). This step is also depicted to a minor extent (30%) by FRET between $IF1_4$(Atto540Q) and $30S_{S13}$(Alx488), explaining why the replacement of GTP with GTPγS only partially hinders the reaction (Figure 3E).

All subsequent steps of the reaction pathway are inhibited when GTP hydrolysis is prevented. The sequence of the following steps is assigned on the basis of their kinetics, in particular by the characteristic duration of the delay phase (Supplementary Figure S2). Single-turnover Pi release corresponds to the step D→E (k_4). The subsequent rounds of multiple-turnover GTP hydrolysis and Pi release, uncoupled from initiation, are described by a late, very slow step I→J (k_9), the rate of which was assigned a fixed value of 0.01 s^{-1}. Bpy-Met-$tRNA^{fMet}$ release from IF2 is given by E→F (k_5). IF1 and IF2 dissociation from the 70S IC, and GDP release from IF2 – reported by the major phase of FRET between $IF1_4$(Atto540Q) and $30S_{S13}$(Alx488), the second phase of FRET between mant-GTP and IF2, and the fluorescence changes of Bpy-GTP, respectively – occur at about the same time and are described by a single step F→G (k_6). The final step of fMet-Phe formation (G→H) corresponds to k_7.

An additional step described by k_8 was included in the model to account for the minor phase observed at late time points of the reactions. This step can be explained by slow 50S joining to incorrectly formed or 'inactive' (51) 30S ICs and is observed predominantly in the presence of IF3 which confers an anti-association conformation on these complexes. All reactions occurring after subunit joining were assumed to be quasi-irreversible, which is very likely for the release reactions (of Pi, IF1, IF2, GDP), and represents a simplification of the model, justified by the commitment of 70S complex in the forward pathway towards maturation and the absence of any evidence for significantly reversible steps. Fitting the data with alternative models, i.e. with a larger number of steps or a different order of events, did not yield satisfactory solutions. The elemental rate constants are summarized in Table 2, and the overall statistics of the fits as well as the contribution of every step to the total fluorescence/FRET change of each observable are presented in Supplementary Figure S7.

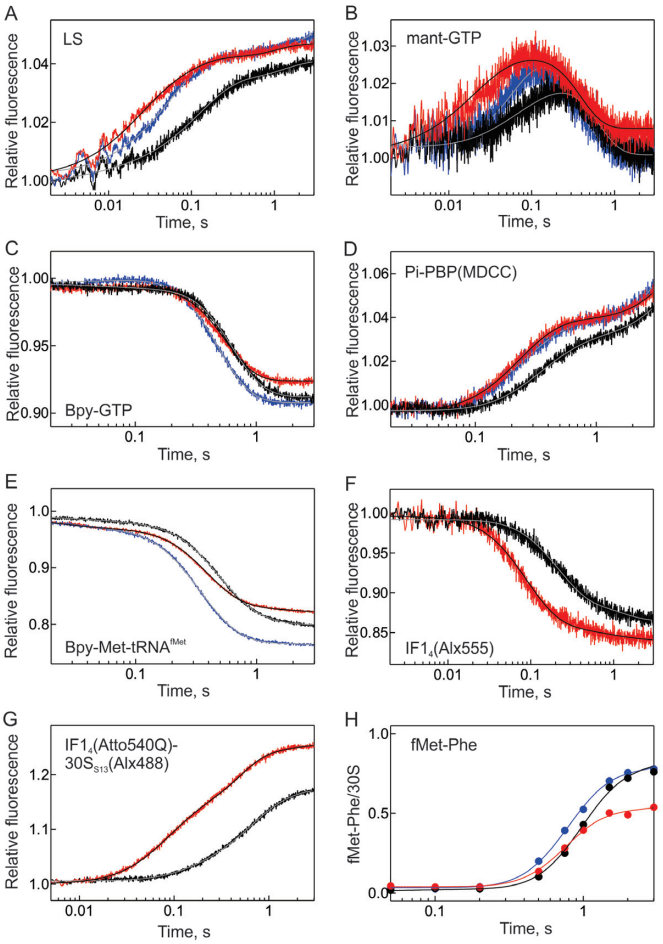

Figure 4. Interplay between initiation factors on the 70S IC. 30S IC containing all initiation factors (black), without IF1 (blue), or without IF3 (red), was rapidly mixed with 50S subunits (1 μM) in a stopped-flow (**A**–**G**) or a quench-flow (**H**) machine and the indicated reactions were monitored. Smooth lines show fits obtained by global evaluation of all time courses using numerical integration.

Role of IF1 and IF3 after 50S subunit joining

To study the individual roles of IF1 and IF3 in promoting each step of 70S IC maturation, the reactions were monitored in the presence and absence of either factor at a fixed concentration (1 μM) of 50S subunits (Figure 4). LS was monitored at increasing concentrations of 50S subunits (Supplementary Figure S1B) to obtain the elemental rate constants of the first step of subunit joining. The time courses were fitted using the model described above, with the exception that IF1-dependent steps were removed from the reaction scheme when IF1 was absent. Numerical integration analysis revealed that the GTPase activation step (monitored by the first phase of FRET changes between

mant-GTP and IF2), which in the full system is a kinetically discrete reaction, in the absence of IF3 becomes indistinguishable from the 50S subunit docking; hence, the two steps were grouped. When the complexes were prepared in the absence of either IF1 or IF3, IF2 dissociation from the 70S complex (as reported by the second phase of FRET between mant-GTP and IF2) occurred at about the same time as the release of $tRNA^{fMet}$ from IF2 (Table 2).

In the absence of IF1 or IF3, the association rate constant of 50S joining was ~40–55 μM^{-1} s^{-1} (Figure 4A, Table 2) and the reaction was almost irreversible (Table 2). The faster subunit joining (Figure 4A, Supplementary Figure S1B, Table 1) also resulted in an increased apparent rate of GTPase activation (Figure 4B, Table 1). However, the elemental rate constant of the reaction did not change in the absence of IF1, while in the absence of IF3 the rate was faster than the preceding step (Table 2). Omitting IF1 or IF3 from the 30S IC did not influence the efficiency of IF2-dependent reactions such as the release of GDP and Pi (Figure 4C and D, respectively). In the absence of IF3, a moderate decrease in the extent (20–40%) of Bpy-Met-$tRNA^{fMet}$ fluorescence change (Figure 4E) and peptide bond formation (Figure 4H) was observed. When IF1 or IF3 were absent, the rates of Pi release remained unaffected, whereas $tRNA^{fMet}$ release from IF2 was slightly slower with IF2 dissociation occurring in parallel. Subsequently, under these conditions, GDP release and peptide bond formation became slightly faster (Table 2). Overall, the IF2 pathway followed the same sequence of events, regardless of the presence of IF1 or IF3 (Supplementary Figure S2B-C).

When IF3 was omitted from the complex, the apparent rate of the IF1 environment change (depicted by $IF1_4$(Alx555) fluorescence) was 2-fold faster due to faster subunit joining (Figure 4F, Table 1). Under these conditions, a significant proportion (~50%) of the amplitude of FRET between $IF1_4$(Atto540Q) and $30S_{S13}$(Alx488) was ascribed to the change in IF1 environment, whereas the remaining half was due to IF1 dissociation (Figure 4G). Also the overall amplitude of the IF1 signal change was larger, presumably because rapid and irreversible subunit joining occurs even with incorrectly formed 30S complexes which, in the complete system, are strongly discriminated against by IF3. We checked whether the absence of IF1 affected the IF3 dynamics by monitoring FRET between $IF3_{166}$(Alx555) and fluorescein-labeled fMet-$tRNA^{fMet}$ (21), and observed that the apparent rate of IF3 dissociation from such complexes was 3-fold faster (Table 1, Supplementary Figure S6), which can be similarly attributed to the faster subunit joining. In summary, despite the observed differences in the time courses of different reactions, the only step that is significantly affected by the absence of IF1 or IF3 is 50S subunit joining.

Reversibility of the initiation pathway

To further examine the role of GTP hydrolysis, we investigated whether a mature 70S IC can recruit IF1 and IF2 when GTP is replaced with GTPγS. As noted above, when 30S IC formed with GTP and Bpy-Met-$tRNA^{fMet}$ was rapidly mixed with 50S subunits, a decrease in Bpy fluorescence was observed due to the release of Bpy-Met-$tRNA^{fMet}$ from IF2 following GTP hydrolysis (Figures 2E and 5A). When the same experiment was performed in the presence of a 20-fold excess of GTPγS, added along with the 50S subunits, a biphasic fluorescence change was observed (Figure 5A). The initial decrease in signal was followed by an increase in fluorescence caused by re-binding of IF2, after the exchange of GDP for GTPγS, to the mature 70S IC and subsequent capture of the 3′ CCA-end of Bpy-Met-$tRNA^{fMet}$ by IF2–GTPγS. Thus, in the absence of GTP hydrolysis, the binding equilibrium is shifted towards the formation of the Bpy-Met-$tRNA^{fMet}$–IF2–70S complex and the dissociation of IF2 is disfavored, thereby preventing the formation of the mature 70S IC which can enter the elongation phase.

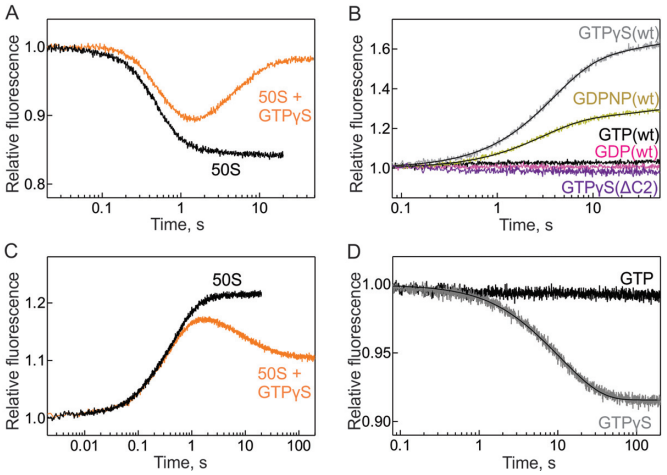

Figure 5. Effect of GTP hydrolysis on binding of IF1 and IF2 to mature 70S IC. (**A**) 30S IC formed in the presence of Bpy-Met-$tRNA^{fMet}$ and GTP (12.5 μM) was rapidly mixed with 50S subunits in the presence or absence of GTPγS (0.25 mM). Time courses of Bpy-Met-$tRNA^{fMet}$ fluorescence changes were monitored. (**B**) Interaction of Bpy-Met-$tRNA^{fMet}$ with IF2 upon binding of the factor to 70S IC was followed by mixing purified 70S ICs (containing Bpy-Met-$tRNA^{fMet}$) with IF2 bound to GTPγS, GDPNP, GTP or GDP. Similar experiments were performed using an IF2 variant lacking the C2-domain (ΔC2) in the presence of GTPγS. (**C**) $30S_{S13}$(Alx488) IC formed with $IF1_4$(Atto540Q) and GTP (12.5 μM) was mixed with 50S subunits in the presence or absence of GTPγS (0.25 mM). (**D**) The binding of the IF1 to mature 70S IC was followed by mixing non-purified 70S ICs (formed with $30S_{S13}$(Alx488) in the absence of IF1) with $IF1_4$(Atto540Q), in the presence of GTP or GTPγS.

To further substantiate these findings, we mixed purified 70S ICs containing Bpy-Met-$tRNA^{fMet}$ with IF2 bound to GTPγS or GDPNP (Figure 5B). The observed fluorescence increase depicts the binding of IF2 to Bpy-Met-$tRNA^{fMet}$ on the ribosome. When a truncated version of IF2, lacking the C2-domain (64), was used together with GTPγS, no fluorescence change was observed, confirming the loss of the direct interaction between $tRNA^{fMet}$ and IF2. Additionally, no fluorescence increase occurred upon binding of the full-length IF2 to 70S IC–Bpy-Met-$tRNA^{fMet}$ in the presence of GTP, owing to rapid GTP hydrolysis and IF2 dissociation. Control experiments performed in the presence of GDP also showed no fluorescence change (Figure 5B).

Similarly, when $30S_{S13}$(Alx488) IC, formed with GTP and $IF1_4$(Atto540Q), was rapidly mixed with 50S subunits, an increase in fluorescence was observed upon release of

$IF1_4$(Atto540Q) from the 70S complex (Figures 2G and 5C). In the presence of a 20-fold excess of GTPγS added along with the 50S subunits, a biphasic fluorescence change was observed (Figure 5C) representing the initial release of IF1, followed by rebinding of the factor to the 70S complex. We checked whether IF1 could bind to preformed 70S ICs by mixing unpurified $70S_{S13}$(Alx488) IC (which contained IF2 in solution) with $IF1_4$(Atto540Q) in the presence of GTP or GTPγS (Figure 5D). No binding was observed in the presence of GTP, whereas IF1 could bind to mature 70S complexes in the presence of GTPγS.

Because IF2 is the effector molecule which binds the guanine nucleotide, it appears that the binding of IF1 to the 70S IC is promoted by the interaction of IF2 in the pre-hydrolysis state with the 70S complex. On the 30S IC, IF1 may contact the NTD (N-terminal domain) of the α-form (i.e. containing the full-length NTD) of *E. coli* IF2 (27). To test whether the interplay between IF1 and IF2 is specific to this particular isoform of IF2, we checked whether IF1 release can be uncoupled from GTP hydrolysis and consequent IF2 dissociation by using a truncated version of IF2 lacking the entire NTD (IF2 ΔN (41)) (Supplementary Figure S8). In the absence of GTP hydrolysis by IF2ΔN, $IF1_4$(Atto540Q) was not released from the $70S_{S13}$(Alx488) complex, suggesting that IF1 release from the 70S complex is not mediated by the loss of interaction with the NTD of IF2. Thus, it is possible that (i) IF1 interacts with a different domain of IF2 on the 70S IC, or (ii) IF2 binding to the 70S IC, in the presence of non-hydrolyzable GTP analogs, confers a pre-hydrolysis conformation on the 70S complex, revealing an IF1 binding site. Hence, GTP hydrolysis may guide transition of the 70S IC into an elongation-competent state by rendering the dissociation of IF2 and IF1 from the ribosome irreversible.

DISCUSSION

The present kinetic analysis provides a detailed mechanistic picture of the maturation of the canonical 30S IC to the 70S EC (Figure 6). 50S subunit joining is the first step towards the formation of the 70S complex. When all factors, fMet-$tRNA^{fMet}$, and GTP are bound to the 30S subunit carrying the 022 mRNA, subunit joining occurs with an apparent rate constant of 15 $\mu M^{-1}\ s^{-1}$ (21). However, the detailed kinetic analysis, which takes into account the steps following 50S subunit joining, indicates that the initial 50S subunit docking is reversible with elemental rate constants of about $k_1 = 30\ \mu M^{-1}s^{-1}$ and $k_{-1} = 30\ s^{-1}$, consistent with previously published results (20). The 70S PIC intermediate formed immediately upon 50S subunit joining (Figure 6) may correspond to the short-lived state of the 70S complex observed by single-molecule FRET (15). Further rearrangements of the complex are required to stabilize the interaction between the two subunits, leading to the formation of the 70S IC (15,20). When mRNAs containing a non-optimal TIR are used, the initial 50S subunit docking is not inhibited, whereas the transition toward stable 70S IC formation is very slow due to the high dissociation rate of the complex and slow transitions towards the 70S EC (21,29).

Subunit joining is followed by rapid GTPase activation of IF2 (36 s^{-1}) and GTP hydrolysis (19,20), along with subsequent conformational rearrangements resulting in a change of IF1 environment (21 s^{-1}). Pi release (~4 s^{-1}), which occurs after GTP hydrolysis, is followed by the rapid release of fMet-$tRNA^{fMet}$ from IF2 (18 s^{-1}), leading to tRNA accommodation in the P site (33,34,65). Previous reports showed that $tRNA^{fMet}$ conformational changes, monitored by the fluorescence change of proflavin attached to the D-loop of fMet-$tRNA^{fMet}$, precede Pi release (20). We were unable to model our datasets with Bpy-Met-$tRNA^{fMet}$ to suit this sequence of events, suggesting that the two labels may report on two different $tRNA^{fMet}$-dependent reactions. Thereafter, IF2 and IF1 dissociate from the 70S complex (6 s^{-1}), and IF2 exchanges its bound GDP for GTP to participate in further initiation events. Because the affinity of GDP and GTP to free IF2 is similar under physiological conditions (58), the nucleotide exchange occurs spontaneously due to a high rate of GDP dissociation and a high cellular concentration of GTP in the cell (53). Lastly, peptide bond formation occurs after a 300 ms lag phase with the elemental rate constant of 2.3 s^{-1} (21). The delay represents the time required for the formation of 70S IC. When a pre-formed 70S IC is used instead of the 30S IC and 50S subunits, no delay phase is observed and the time courses of peptide bond formation are single-exponential with a rate constant of 2 s^{-1} (21,66). IF3 dissociation (3.2 s^{-1}) takes place concomitantly with the maturation of the 70S complex (21) and is independent of GTP hydrolysis.

In the absence of either IF1 or IF3, subunit association is slightly faster than in the presence of the two factors (elemental rate constants are 40–50 $\mu M^{-1}s^{-1}$), but the dissociation of these complexes is very slow (Table 2), giving rise to the overall higher apparent rate constants of the reaction (~40 $\mu M^{-1}s^{-1}$). The low rates of subunit dissociation indicate the formation of a longer-lived complex, explaining how IF1 and IF3 can contribute to mRNA selection at the 50S subunit association step (15,21). The faster subunit joining results in higher rates of GTPase activation, change in IF1 environment, and IF3 dissociation, without affecting the elemental rate constants of the reactions. Notably, the 50S subunit joining is the only step in the late initiation pathway that is influenced by the absence of IF1 or IF3, whereas none of the following steps are significantly affected.

The timing and extent of subunit joining are entirely independent of GTP hydrolysis by IF2 (23,36,63). However, the lack of GTP hydrolysis hinders the IF2-dependent reactions such as the dissociation of $tRNA^{fMet}$ from the C2-domain of IF2 and peptide bond formation (20,29,36,65). The utilization of GTPγS conferred a higher degree of inhibition than was previously reported in the presence of a different non-hydrolyzable GTP analog, GDPCP (20,29), or GDP/no nucleotide (19). In the former case, the authors (20,29) observed a 2–3-fold reduction in the amplitude of $tRNA^{fMet}$ conformational changes and dipeptide formation, events that are almost completely inhibited in our system. We checked subunit joining and $tRNA^{fMet}$ release from IF2 in the presence of the same analog, GDPCP, and found very little differences when compared to GTPγS (data not shown). We also observed that the rate of subunit joining in the presence of GDP or in the absence of any nucleotide (0.02 s^{-1}) was >200-fold slower than in the presence of GTP

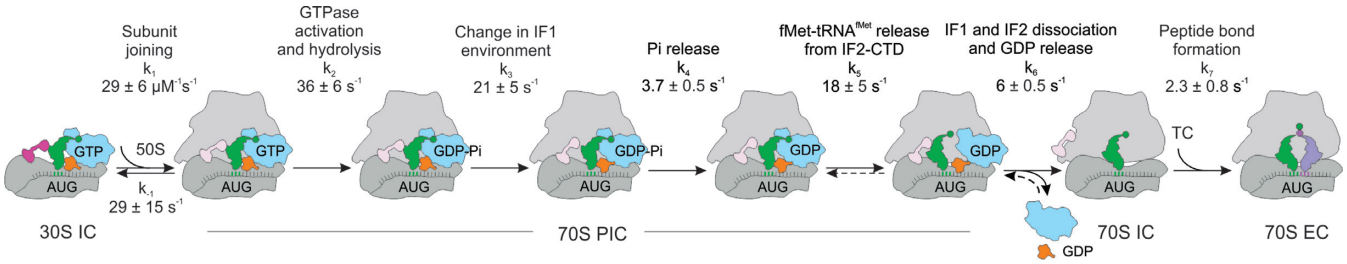

Figure 6. Detailed kinetic scheme of late events in bacterial translation initiation. IF1, IF2–GTP, IF3, mRNA and fMet-tRNA^{fMet} bind the 30S subunit to form a 30S IC. Step 1: Association of the 50S subunit to 30S IC to form a 70S PIC. Step 2: GTPase activation and rapid GTP hydrolysis (19,20,23,32). Step 3: Change of IF1 environment. Step 4: Pi release from IF2. Step 5: Release of the 3′ end of fMet-tRNA^{fMet} from IF2 C2-domain. Step 6: Release of IF2 from the 70S complex and GDP from IF2; release of IF1 from the 70S complex, giving rise to an elongation competent 70S IC. Step 7: Binding of EF-Tu–GTP–aminoacyl-tRNA (TC) to the 70S IC is followed by peptide bond formation to form a 70S EC. Dissociation of IF3 from the 70S complex was reported to proceed at an apparent rate of 3.2 s^{-1} (21); because IF3 may undergo conformational changes and movements while the complex maturates, the position of IF3 is indicated by a lighter shade and should be considered tentative. Dissociation of IF1 and IF2 to 70S IC, as well as step 5, become reversible in the absence of GTP hydrolysis, as indicated by dashed arrows. The observables employed to monitor each step are summarized in Table 2.

(data not shown), in agreement with earlier reports (62). These results suggest that the discrepancy most likely arises from differences in the susceptibility of IF2 from *E. coli* (our system) or from *G. stearothermophilus* (used in (19,20,29)) for different guanine nucleotides. In the presence of GTPγS, IF2 could bind to the 3′ end of fMet-tRNA^{fMet} on a mature 70S IC and the equilibrium of the reaction was shifted towards the pre-hydrolysis state of complex formation, suggesting an important role of GTP hydrolysis in promoting the directionality of late stages of translation initiation.

It remains unknown whether Pi release is an obligatory step for the release of fMet-tRNA^{fMet} from IF2. In case of EF-G, Pi release and tRNA-mRNA translocation can take place independently of one another (67); a similar mechanism may apply to Pi and fMet-tRNA^{fMet} release from IF2. If the two factors employ a similar coupling mechanism, then a step preceding Pi release and tRNA dissociation from IF2 may be rate-limiting for the remaining part of the IF2 pathway. On the other hand, if Pi release is necessary for fMet-tRNA^{fMet} dissociation from IF2, it would imply that the G-domain can convey conformational changes to the C2-domain. It is not clear how GTP hydrolysis or Pi release from the G-domain can be communicated to the C2-domain of IF2. While structural work on the eukaryotic/archaeal IF2 homolog, e/aIF5B, suggested that the nucleotide binding status of the molecule may be communicated through the inter-domain interface (60,68), IF2 might not use the same mechanism because of the different arrangement of its domains (69,70). Pi and tRNA^{fMet} release from IF2 promote dissociation of the factor from the ribosome via (i) the conformational rearrangement of IF2 from its high-affinity state on the 70S complex to its low-affinity, ready-to-leave GDP conformation (33,34), and (ii) the loss of the direct interaction with the 3′ end of fMet-tRNA^{fMet}, which is an important anchor point for IF2 on the ribosome (26,33). In fact, it has been observed that a lower affinity of IF2 towards fMet-tRNA^{fMet} ((1); Goyal et al., unpublished data) or the ribosome (52,71) can help bypass the requirement for GTP hydrolysis in promoting IF2 release from the 70S complex.

The absence of IF1 does not significantly affect the extent or the timing of IF2-dependent reactions on the 70S complex. On the other hand, the lack of GTP hydrolysis by IF2 abolishes the dissociation of IF1 from the ribosome. Similar results were obtained using a reconstituted system from *Saccharomyces cerevisiae,* where the dissociation of eIF1A (the eukaryotic homolog of IF1) from the 80S IC was shown to be 10-fold slower in the absence of GTP hydrolysis by eIF5B (72). Once released, IF1 can rebind only to the pre-hydrolysis state of the ribosome (e.g. induced by IF2–GTPγS). It is unclear which of the several IF2-dependent events, such as GTP hydrolysis, Pi release, fMet-tRNA^{fMet} release, intersubunit rotation, or the dissociation of IF2 from the ribosome, is directly responsible for promoting the release of IF1 from the 70S IC. Because the dependence of IF1 release from the 70S complex on GTP hydrolysis is not eliminated by using an IF2 variant lacking the NTD, it is likely that the release of IF1 is dependent on GTP hydrolysis even in those organisms in which IF2 does not retain its full-length NTD. The dissociation of IF1 from the 70S complex may be promoted by the loss of direct interaction with IF2 or conformational rearrangements of the ribosome that occur after GTP hydrolysis, explaining the faster rate of IF1 release from 70S IC, as compared with 30S IC (apparent rate of 2 s^{-1} versus 0.01 s^{-1}, respectively (Supplementary Figure S5B)).

In contrast to IF1, the dissociation of IF3 from the 70S IC is not affected when GTP hydrolysis is prevented. These findings are at variance with the suggestion that GTP hydrolysis may be required for IF3 release from the 70S complex (33). It is possible, however, that the step we have assigned to IF3 dissociation (21), may represent a major movement of IF3, e.g. away from the subunit interface and towards the outer surface of the ribosome, which would free bridge B2b (27,28,73,74) together with other intersubunit bridges (38), and allow stable subunit joining to take place.

The frequency with which a given mRNA enters translation is dependent on the assembly of a 30S IC with a favorable conformation which promotes facile binding of the 50S subunit (13,21). IF1 and IF3 act as gate-keepers during early stages of initiation by preventing subunit docking to unproductive 30S ICs and favoring a stage in initiation during which the 50S subunit docking is reversible (15,21,29). After stable subunit joining, this checkpoint is crossed and the mRNA can no longer freely dissociate from the complex. On the correctly-formed 30S IC, IF1 and IF3 predom-

inantly exert control over 70S IC maturation by regulating the rate of 50S subunit docking and dissociation. However, it is not excluded that IF1 and IF3 may carry out additional fidelity functions at the 70S IC level during translation initiation of mRNAs containing a non-canonical TIR. Thus, the progression from the 30S IC to the elongating ribosome proceeds through a sequence of steps which couple the quality control by IF3/IF1 and IF2-dependent GTP hydrolysis to a stepwise release of the initiation factors and the tightening of the association between the subunits.

SUPPLEMENTARY DATA

Supplementary Data are available at NAR Online.

ACKNOWLEDGEMENT

We thank Wolfgang Wintermeyer for critically reading the manuscript; Liudmila Filonava for conducting initial experiments; Dmitry Burakovsky and Irena Andreeva for providing additional preparations of ribosomal subunits and Bpy-Met-tRNA^{fMet}, respectively; and Olaf Geintzer, Sandra Kappler, Christina Kothe, Anna Pfeifer, Theresia Uhlendorf, Tanja Wiles, and Michael Zimmermann for expert technical assistance.

FUNDING

Boehringen Ingelheim Fonds and the Göttingen Graduate School for Neurosciences, Biophysics, and Molecular Biosciences (to A.G.); Max Planck Society and grants of the Deutsche Forschungsgemeinschaft (to M.V.R.); Peruvian Programa Nacional de Innovación para la Competitividad y Productividad [382-PNICP-PIBA-2014 (to P.M.)]. Funding for open access charge: Max Planck Society.
Conflict of interest statement. None declared.

REFERENCES

1. Gualerzi,C.O., Brandi,L., Caserta,E., Garofalo,C., Lammi,M., La Teana,A., Petrelli,D., Spurio,R., Tomsic,J. and Pon,C.L. (2001) Initiation factors in the early events of mRNA translation in bacteria. *Cold Spring Harb. Symp. Quant. Biol.*, **66**, 363–376.
2. Boelens,R. and Gualerzi,C.O. (2002) Structure and function of bacterial initiation factors. *Curr. Protein Pept. Sci.*, **3**, 107–119.
3. Myasnikov,A.G., Simonetti,A., Marzi,S. and Klaholz,B.P. (2009) Structure-function insights into prokaryotic and eukaryotic translation initiation. *Curr. Opin. Struct. Biol.*, **19**, 300–309.
4. Simonetti,A., Marzi,S., Jenner,L., Myasnikov,A., Romby,P., Yusupova,G., Klaholz,B.P. and Yusupov,M. (2009) A structural view of translation initiation in bacteria. *Cell. Mol. Life Sci.*, **66**, 423–436.
5. Laursen,B.S., Sorensen,H.P., Mortensen,K.K. and Sperling-Petersen,H.U. (2005) Initiation of protein synthesis in bacteria. *Microbiol. Mol. Biol. Rev.*, **69**, 101–123.
6. Milon,P. and Rodnina,M.V. (2012) Kinetic control of translation initiation in bacteria. *Crit. Rev. Biochem. Mol. Biol.*, **47**, 334–348.
7. Allen,G.S. and Frank,J. (2007) Structural insights on the translation initiation complex: ghosts of a universal initiation complex. *Mol. Microbiol.*, **63**, 941–950.
8. Zucker,F.H. and Hershey,J.W. (1986) Binding of Escherichia coli protein synthesis initiation factor IF1 to 30S ribosomal subunits measured by fluorescence polarization. *Biochemistry*, **25**, 3682–3690.
9. Weiel,J. and Hershey,J.W. (1982) The binding of fluorescein-labeled protein synthesis initiation factor 2 to Escherichia coli 30 S ribosomal subunits determined by fluorescence polarization. *J. Biol. Chem.*, **257**, 1215–1220.
10. Stringer,E.A., Sarkar,P. and Maitra,U. (1977) Function of initiation factor 1 in the binding and release of initiation factor 2 from ribosomal initiation complexes in Escherichia coli. *J. Biol. Chem.*, **252**, 1739–1744.
11. Celano,B., Pawlik,R.T. and Gualerzi,C.O. (1988) Interaction of Escherichia coli translation-initiation factor IF-1 with ribosomes. *Eur. J. Biochem.*, **178**, 351–355.
12. Caserta,E., Tomsic,J., Spurio,R., La Teana,A., Pon,C.L. and Gualerzi,C.O. (2006) Translation initiation factor IF2 interacts with the 30 S ribosomal subunit via two separate binding sites. *J. Mol. Biol.*, **362**, 787–799.
13. Milon,P., Maracci,C., Filonava,L., Gualerzi,C.O. and Rodnina,M.V. (2012) Real-time assembly landscape of bacterial 30S translation initiation complex. *Nat. Struct. Mol. Biol.*, **19**, 609–615.
14. Wang,J., Caban,K. and Gonzalez,R.L. Jr (2015) Ribosomal initiation complex-driven changes in the stability and dynamics of initiation factor 2 regulate the fidelity of translation initiation. *J. Mol. Biol.*, **427**, 1819–1834.
15. MacDougall,D.D. and Gonzalez,R.L. Jr (2015) Translation initiation factor 3 regulates switching between different modes of ribosomal subunit joining. *J. Mol. Biol.*, **427**, 1801–1818.
16. Guenneugues,M., Caserta,E., Brandi,L., Spurio,R., Meunier,S., Pon,C.L., Boelens,R. and Gualerzi,C.O. (2000) Mapping the fMet-tRNA(f)(Met) binding site of initiation factor IF2. *EMBO J.*, **19**, 5233–5240.
17. Milon,P., Carotti,M., Konevega,A.L., Wintermeyer,W., Rodnina,M.V. and Gualerzi,C.O. (2010) The ribosome-bound initiation factor 2 recruits initiator tRNA to the 30S initiation complex. *EMBO Rep.*, **11**, 312–316.
18. Spurio,R., Brandi,L., Caserta,E., Pon,C.L., Gualerzi,C.O., Misselwitz,R., Krafft,C., Welfle,K. and Welfle,H. (2000) The C-terminal subdomain (IF2 C-2) contains the entire fMet-tRNA binding site of initiation factor IF2. *J. Biol. Chem.*, **275**, 2447–2454.
19. Tomsic,J., Vitali,L.A., Daviter,T., Savelsbergh,A., Spurio,R., Striebeck,P., Wintermeyer,W., Rodnina,M.V. and Gualerzi,C.O. (2000) Late events of translation initiation in bacteria: a kinetic analysis. *EMBO J.*, **19**, 2127–2136.
20. Grigoriadou,C., Marzi,S., Kirillov,S., Gualerzi,C.O. and Cooperman,B.S. (2007) A quantitative kinetic scheme for 70 S translation initiation complex formation. *J. Mol. Biol.*, **373**, 562–572.
21. Milon,P., Konevega,A.L., Gualerzi,C.O. and Rodnina,M.V. (2008) Kinetic checkpoint at a late step in translation initiation. *Mol. Cell*, **30**, 712–720.
22. Marshall,R.A., Aitken,C.E. and Puglisi,J.D. (2009) GTP hydrolysis by IF2 guides progression of the ribosome into elongation. *Mol. Cell*, **35**, 37–47.
23. Qin,H., Grigoriadou,C. and Cooperman,B.S. (2009) Interaction of IF2 with the ribosomal GTPase-associated center during 70S initiation complex formation. *Biochemistry*, **48**, 4699–4706.
24. Antoun,A., Pavlov,M.Y., Lovmar,M. and Ehrenberg,M. (2006) How initiation factors tune the rate of initiation of protein synthesis in bacteria. *EMBO J.*, **25**, 2539–2550.
25. Grunberg-Manago,M., Dessen,P., Pantaloni,D., Godefroy-Colburn,T., Wolfe,A.D. and Dondon,J. (1975) Light-scattering studies showing the effect of initiation factors on the reversible dissociation of Escherichia coli ribosomes. *J. Mol. Biol.*, **94**, 461–478.
26. Simonetti,A., Marzi,S., Myasnikov,A.G., Fabbretti,A., Yusupov,M., Gualerzi,C.O. and Klaholz,B.P. (2008) Structure of the 30S translation initiation complex. *Nature*, **455**, 416–420.
27. Julian,P., Milon,P., Agirrezabala,X., Lasso,G., Gil,D., Rodnina,M.V. and Valle,M. (2011) The Cryo-EM structure of a complete 30S translation initiation complex from Escherichia coli. *PLoS Biol.*, **9**, e1001095.
28. Dallas,A. and Noller,H.F. (2001) Interaction of translation initiation factor 3 with the 30S ribosomal subunit. *Mol. Cell*, **8**, 855–864.
29. Grigoriadou,C., Marzi,S., Pan,D., Gualerzi,C.O. and Cooperman,B.S. (2007) The translational fidelity function of IF3 during transition from the 30 S initiation complex to the 70 S initiation complex. *J. Mol. Biol.*, **373**, 551–561.
30. Qin,D. and Fredrick,K. (2009) Control of translation initiation involves a factor-induced rearrangement of helix 44 of 16S ribosomal RNA. *Mol. Microbiol.*, **71**, 1239–1249.

31. Belotserkovsky,J.M., Dabbs,E.R. and Isaksson,L.A. (2011) Mutations in 16S rRNA that suppress cold-sensitive initiation factor 1 affect ribosomal subunit association. *FEBS J.*, **278**, 3508–3517.
32. Huang,C., Mandava,C.S. and Sanyal,S. (2010) The ribosomal stalk plays a key role in IF2-mediated association of the ribosomal subunits. *J. Mol. Biol.*, **399**, 145–153.
33. Allen,G.S., Zavialov,A., Gursky,R., Ehrenberg,M. and Frank,J. (2005) The cryo-EM structure of a translation initiation complex from Escherichia coli. *Cell*, **121**, 703–712.
34. Myasnikov,A.G., Marzi,S., Simonetti,A., Giuliodori,A.M., Gualerzi,C.O., Yusupova,G., Yusupov,M. and Klaholz,B.P. (2005) Conformational transition of initiation factor 2 from the GTP- to GDP-bound state visualized on the ribosome. *Nat. Struct. Mol. Biol.*, **12**, 1145–1149.
35. Luchin,S., Putzer,H., Hershey,J.W., Cenatiempo,Y., Grunberg-Manago,M. and Laalami,S. (1999) In vitro study of two dominant inhibitory GTPase mutants of Escherichia coli translation initiation factor IF2. Direct evidence that GTP hydrolysis is necessary for factor recycling. *J. Biol. Chem.*, **274**, 6074–6079.
36. Antoun,A., Pavlov,M.Y., Andersson,K., Tenson,T. and Ehrenberg,M. (2003) The roles of initiation factor 2 and guanosine triphosphate in initiation of protein synthesis. *EMBO J.*, **22**, 5593–5601.
37. Lockwood,A.H., Sarkar,P. and Maitra,U. (1972) Release of polypeptide chain initiation factor IF-2 during initiation complex formation. *Proc. Natl. Acad. Sci. U.S.A.*, **69**, 3602–3605.
38. Fabbretti,A., Pon,C.L., Hennelly,S.P., Hill,W.E., Lodmell,J.S. and Gualerzi,C.O. (2007) The real-time path of translation factor IF3 onto and off the ribosome. *Mol. Cell*, **25**, 285–296.
39. Elvekrog,M.M. and Gonzalez,R.L. Jr (2013) Conformational selection of translation initiation factor 3 signals proper substrate selection. *Nat. Struct. Mol. Biol.*, **20**, 628–633.
40. Boileau,G., Butler,P., Hershey,J.W. and Traut,R.R. (1983) Direct cross-links between initiation factors 1, 2, and 3 and ribosomal proteins promoted by 2-iminothiolane. *Biochemistry*, **22**, 3162–3170.
41. Moreno,J.M., Drskjotersen,L., Kristensen,J.E., Mortensen,K.K. and Sperling-Petersen,H.U. (1999) Characterization of the domains of E. coli initiation factor IF2 responsible for recognition of the ribosome. *FEBS Lett.*, **455**, 130–134.
42. Milon,P., Konevega,A.L., Peske,F., Fabbretti,A., Gualerzi,C.O. and Rodnina,M.V. (2007) Transient kinetics, fluorescence, and FRET in studies of initiation of translation in bacteria. *Methods Enzymol.*, **430**, 1–30.
43. Rodnina,M.V. and Wintermeyer,W. (1995) GTP consumption of elongation factor Tu during translation of heteropolymeric mRNAs. *Proc. Natl. Acad. Sci. U.S.A.*, **92**, 1945–1949.
44. Rodnina,M.V., Fricke,R. and Wintermeyer,W. (1994) Transient conformational states of aminoacyl-tRNA during ribosome binding catalyzed by elongation factor Tu. *Biochemistry*, **33**, 12267–12275.
45. Caliskan,N., Katunin,V.I., Belardinelli,R., Peske,F. and Rodnina,M.V. (2014) Programmed -1 frameshifting by kinetic partitioning during impeded translocation. *Cell*, **157**, 1619–1631.
46. Cunha,C.E., Belardinelli,R., Peske,F., Holtkamp,W., Wintermeyer,W. and Rodnina,M.V. (2013) Dual use of GTP hydrolysis by elongation factor G on the ribosome. *Translation*, **1**, e24315.
47. Brune,M., Hunter,J.L., Corrie,J.E. and Webb,M.R. (1994) Direct, real-time measurement of rapid inorganic phosphate release using a novel fluorescent probe and its application to actomyosin subfragment 1 ATPase. *Biochemistry*, **33**, 8262–8271.
48. Holtkamp,W., Cunha,C.E., Peske,F., Konevega,A.L., Wintermeyer,W. and Rodnina,M.V. (2014) GTP hydrolysis by EF-G synchronizes tRNA movement on small and large ribosomal subunits. *EMBO J.*, **33**, 1073–1085.
49. Gite,S., Mamaev,S., Olejnik,J. and Rothschild,K. (2000) Ultrasensitive fluorescence-based detection of nascent proteins in gels. *Anal. Biochem.*, **279**, 218–225.
50. Wishnia,A., Boussert,A., Graffe,M., Dessen,P.H. and Grunberg-Manago,M. (1975) Kinetics of the reversible association of ribosomal subunits: stopped-flow studies of the rate law and of the effect of Mg2+. *J. Mol. Biol.*, **93**, 499–415.
51. McGinnis,J.L., Liu,Q., Lavender,C.A., Devaraj,A., McClory,S.P., Fredrick,K. and Weeks,K.M. (2015) In-cell SHAPE reveals that free 30S ribosome subunits are in the inactive state. *Proc. Natl. Acad. Sci. U.S.A.*, **112**, 2425–2430.
52. Fabbretti,A., Brandi,L., Milon,P., Spurio,R., Pon,C.L. and Gualerzi,C.O. (2012) Translation initiation without IF2-dependent GTP hydrolysis. *Nucleic Acids Res.*, **40**, 7946–7955.
53. Milon,P., Tischenko,E., Tomsic,J., Caserta,E., Folkers,G., La Teana,A., Rodnina,M.V., Pon,C.L., Boelens,R. and Gualerzi,C.O. (2006) The nucleotide-binding site of bacterial translation initiation factor 2 (IF2) as a metabolic sensor. *Proc. Natl. Acad. Sci. U.S.A.*, **103**, 13962–13967.
54. Simonetti,A., Marzi,S., Billas,I.M., Tsai,A., Fabbretti,A., Myasnikov,A.G., Roblin,P., Vaiana,A.C., Hazemann,I., Eiler,D. *et al.* (2013) Involvement of protein IF2 N domain in ribosomal subunit joining revealed from architecture and function of the full-length initiation factor. *Proc. Natl. Acad. Sci. U.S.A.*, **110**, 15656–15661.
55. Rodnina,M.V., Fricke,R., Kuhn,L. and Wintermeyer,W. (1995) Codon-dependent conformational change of elongation factor Tu preceding GTP hydrolysis on the ribosome. *EMBO J.*, **14**, 2613–2619.
56. Daviter,T., Wieden,H.J. and Rodnina,M.V. (2003) Essential role of histidine 84 in elongation factor Tu for the chemical step of GTP hydrolysis on the ribosome. *J. Mol. Biol.*, **332**, 689–699.
57. Maracci,C., Peske,F., Dannies,E., Pohl,C. and Rodnina,M.V. (2014) Ribosome-induced tuning of GTP hydrolysis by a translational GTPase. *Proc. Natl. Acad. Sci. U.S.A.*, **111**, 14418–14423.
58. Hauryliuk,V., Mitkevich,V.A., Draycheva,A., Tankov,S., Shyp,V., Ermakov,A., Kulikova,A.A., Makarov,A.A. and Ehrenberg,M. (2009) Thermodynamics of GTP and GDP binding to bacterial initiation factor 2 suggests two types of structural transitions. *J. Mol. Biol.*, **394**, 621–626.
59. Severini,M., Spurio,R., La Teana,A., Pon,C.L. and Gualerzi,C.O. (1991) Ribosome-independent GTPase activity of translation initiation factor IF2 and of its G-domain. *J. Biol. Chem.*, **266**, 22800–22802.
60. Kuhle,B. and Ficner,R. (2014) eIF5B employs a novel domain release mechanism to catalyze ribosomal subunit joining. *EMBO J.*, **33**, 1177–1191.
61. Paleskava,A., Konevega,A.L. and Rodnina,M.V. (2012) Thermodynamics of the GTP-GDP-operated conformational switch of selenocysteine-specific translation factor SelB. *J. Biol. Chem.*, **287**, 27906–27912.
62. Antoun,A., Pavlov,M.Y., Tenson,T. and Ehrenberg,M.M. (2004) Ribosome formation from subunits studied by stopped-flow and Rayleigh light scattering. *Biol. Proced. Online*, **6**, 35–54.
63. Tsai,A., Petrov,A., Marshall,R.A., Korlach,J., Uemura,S. and Puglisi,J.D. (2012) Heterogeneous pathways and timing of factor departure during translation initiation. *Nature*, **487**, 390–393.
64. Mortensen,K.K., Kildsgaard,J., Moreno,J.M., Steffensen,S.A., Egebjerg,J. and Sperling-Petersen,H.U. (1998) A six-domain structural model for Escherichia coli translation initiation factor IF2. Characterisation of twelve surface epitopes. *Biochem. Mol. Biol. Int.*, **46**, 1027–1041.
65. La Teana,A., Pon,C.L. and Gualerzi,C.O. (1996) Late events in translation initiation. Adjustment of fMet-tRNA in the ribosomal P-site. *J. Mol. Biol.*, **256**, 667–675.
66. Pape,T., Wintermeyer,W. and Rodnina,M.V. (1998) Complete kinetic mechanism of elongation factor Tu-dependent binding of aminoacyl-tRNA to the A site of the E. coli ribosome. *EMBO J.*, **17**, 7490–7497.
67. Savelsbergh,A., Katunin,V.I., Mohr,D., Peske,F., Rodnina,M.V. and Wintermeyer,W. (2003) An elongation factor G-induced ribosome rearrangement precedes tRNA-mRNA translocation. *Mol. Cell*, **11**, 1517–1523.
68. Roll-Mecak,A., Cao,C., Dever,T.E. and Burley,S.K. (2000) X-Ray structures of the universal translation initiation factor IF2/eIF5B: conformational changes on GDP and GTP binding. *Cell*, **103**, 781–792.
69. Eiler,D., Lin,J., Simonetti,A., Klaholz,B.P. and Steitz,T.A. (2013) Initiation factor 2 crystal structure reveals a different domain organization from eukaryotic initiation factor 5B and mechanism among translational GTPases. *Proc. Natl. Acad. Sci. U.S.A.*, **110**, 15662–15667.
70. Wienk,H., Tishchenko,E., Belardinelli,R., Tomaselli,S., Dongre,R., Spurio,R., Folkers,G.E., Gualerzi,C.O. and Boelens,R. (2012) Structural dynamics of bacterial translation initiation factor IF2. *J. Biol. Chem.*, **287**, 10922–10932.

71. Shin,B.S., Maag,D., Roll-Mecak,A., Arefin,M.S., Burley,S.K., Lorsch,J.R. and Dever,T.E. (2002) Uncoupling of initiation factor eIF5B/IF2 GTPase and translational activities by mutations that lower ribosome affinity. *Cell*, **111**, 1015–1025.
72. Acker,M.G., Shin,B.S., Nanda,J.S., Saini,A.K., Dever,T.E. and Lorsch,J.R. (2009) Kinetic analysis of late steps of eukaryotic translation initiation. *J. Mol. Biol.*, **385**, 491–506.
73. Kipper,K., Hetenyi,C., Sild,S., Remme,J. and Liiv,A. (2009) Ribosomal intersubunit bridge B2a is involved in factor-dependent translation initiation and translational processivity. *J. Mol. Biol.*, **385**, 405–422.
74. Hennelly,S.P., Antoun,A., Ehrenberg,M., Gualerzi,C.O., Knight,W., Lodmell,J.S. and Hill,W.E. (2005) A time-resolved investigation of ribosomal subunit association. *J. Mol. Biol.*, **346**, 1243–1258.